Volume 54 | Number 97 | 18 December 2018 | Pages 13609–13752

ChemComm

Chemical Communications

rsc.li/chemcomm

ISSN 1359-7345

ROYAL SOCIETY OF CHEMISTRY

COMMUNICATION

Xin Zhou *et al.*

An intracellular diamine oxidase triggered hyperpolarized ^{129}Xe magnetic resonance biosensor

ChemComm

COMMUNICATION

Cite this: *Chem. Commun.*, 2018, **54**, 13654

Received 30th September 2018, Accepted 22nd October 2018

DOI: 10.1039/c8cc07822j

rsc.li/chemcomm

An intracellular diamine oxidase triggered hyperpolarized ^{129}Xe magnetic resonance biosensor†

Bin Zhang,‡ Qianni Guo,‡ Qing Luo, Xiaoxiao Zhang, QingBin Zeng, Longhui Zhao, Yaping Yuan, Weiping Jiang, Yunhuang Yang, Maili Liu, Chaohui Ye and Xin Zhou *

Here, a novel method was developed for suppressing ^{129}Xe signals in cucurbit[6]uril (CB6) until the trigger is activated by a specific enzyme. Due to its noncovalent interactions with amino-groups and CB6, putrescine dihydrochloride (Put) was chosen for blocking interactions between ^{129}Xe and CB6. Upon adding diamine oxidase (DAO), Put was released from CB6 and a ^{129}Xe@CB6 Hyper-CEST signal emerged. This proposed ^{129}Xe biosensor was then tested in small intestinal villus epithelial cells.

Magnetic resonance imaging (MRI) is a well-established clinical imaging method because of its excellent tissue penetration, excellent soft tissue contrast, and noninvasive property.[1] Because MRI has disadvantages for the acquisition of molecular information, it has some limitations in disease diagnosis.[2] Stimuli-responsive ^{1}H MRI contrast agents have been used as probes for the detection of molecules,[3] redox conditions,[4] enzymes,[5] and pH of local environments.[6] Generally, ^{1}H MRI contrast agents are normally needed in micromolar or even larger concentrations because paramagnetic contrast agents work by affecting thermal polarization of ^{1}H nuclei in the local environment.

As an attractive alternative to ^{1}H MRI, hyperpolarized (HP) ^{129}Xe nuclear magnetic resonance NMR and MRI are being studied in an increasingly wide range of applications. There is no natural background competing against with an exogenous HP signal of ^{129}Xe. Using spin-exchange optical pumping (SEOP) for ^{129}Xe, signals of ^{129}Xe can be increased by several orders of magnitude.[7] Since the electron cloud of an ^{129}Xe atom is sensitive to the environment,[8] ^{129}Xe NMR can be used for liquid crystal ordering,[9] pH,[10] and temperature changes detection.[11] Detection sensitivity can be further improved by the Hyper chemical exchange saturation transfer (Hyper-CEST) technique.[12] Furthermore, as chemical exchange occurs more quickly than T_1 relaxation in Hyper-CEST, depolarized ^{129}Xe accumulates in the solvent, allowing for indirect but highly sensitive detection.[13]

The hosts of ^{129}Xe can be functionalized variously. Meanwhile, chemical shift becomes an indicator for diverse applications such as analyte detection and marker imaging.[14] Typically, cryptophane-A (Cry-A) and its derivatives are the most studied ^{129}Xe binding cages for these applications.[15] However, the multistep synthesis and extremely low yields of Cry-A and its derivatives hamper their preparation.[16] CB6 has also been reported as an excellent ^{129}Xe host for Hyper-CEST NMR, which is characterized by higher solubility in water and better exchange parameters for Hyper-CEST in comparison with Cry-A.[17] Various CB6 supramolecular host–guest interactions have been thoroughly studied,[18] and the participation of CB6 in protein binding or enzymatic reactions has been explored.[19] Studies were based on competitive binding, and an unexpected inhibition of the ^{129}Xe@CB6 interaction occurred in the presence of excess target. It would be beneficial to combine the well-known host–guest properties of CB6 with HP ^{129}Xe and diseases related biochemical reactions. However, an "OFF–ON" switch for ^{129}Xe@CB6 biosensor for enzyme detection has not been developed.

Here, a new CB6-based biosensor (Scheme 1) that allows for selective and sensitive enzyme detection was developed using ^{129}Xe Hyper-CEST NMR. In order to design a ^{129}Xe@CB6 "OFF–ON" NMR biosensor successfully, the affinity between a substrate and CB6 is required to significantly differ from that of the enzymatic reaction product and CB6. In other words, a strong CB6 binding substrate was converted into a product that cannot bind to CB6 *via* an enzymatic reaction. The ^{129}Xe@CB6 Hyper-CEST response could be suppressed by a strong CB6 binding substrate until its enzymatic oxidation to a product that cannot bind to CB6. Since the binding constant of substrate@CB6 was

State Key Laboratory for Magnetic Resonance and Atomic and Molecular Physics, National Center for Magnetic Resonance in Wuhan, Wuhan Institute of Physics and Mathematics, Chinese Academy of Sciences, Wuhan National Laboratory for Optoelectronics, Huazhong University of Science and Technology (HUST), Wuhan 430071, China. E-mail: xinzhou@wipm.ac.cn

† Electronic supplementary information (ESI) available: Abbreviations; materials; isothermal titration calorimetry (ITC) studies; enzyme assays; NMR studies; ^{129}Xe Hyper-CEST MR images in buffer; cellular Hyper-CEST spectra studies and ^{129}Xe Hyper-CEST MR images in intestinal villus and epithelial cells. See DOI: 10.1039/c8cc07822j

‡ B. Z. and Q. G. contributed equally to this work.

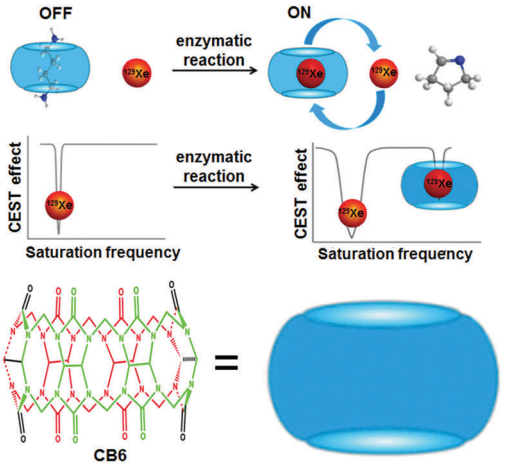

Scheme 1 After the enzymatic reaction, the ^{129}Xe signal in the cage goes from "OFF" to "ON" and the linewidth of ^{129}Xe in solution significantly increases.

much larger than that of ^{129}Xe@CB6, the product of the enzymatic reaction was one that cannot bind to CB6, thus the CEST response emerged after the enzymatic reaction.

As shown in Fig. S1 (ESI†), CB6 (a strong ^{129}Xe binding host) was chosen as a cage of contrast agent. Putrescine dihydrochloride (Put) was chosen as a substrate owing to its strong noncovalent interactions of an amino-group with CB6. For the enzymatic oxidation of Put to aminobutyraldehyde (Ami), diamine oxidase (DAO) was chosen. Then, Ami was converted into an end product (Δ1-pyrroline), which has no amino-group for combining with CB6. After this process, the cavity of CB6 changed from occupied to empty, with the concomitant HP ^{129}Xe exchange inside and outside the cavity. As a result, the NMR signal of the caged ^{129}Xe turned from "OFF to ON".

DAO, playing an important role in polyamines metabolism, is over expressed in small intestinal villus epithelial cells of mammals. An increase in the activity of DAO in serum is closely related to many clinical diseases, including histamine intolerance (HIT), chronic idiopathic urticarial (CIU), small bowel Crohn's disease (SBC), and ruptured fetal membranes.[20] Widely known fluorescence spectrophotometry methods have been developed for DAO.[21] Nevertheless, these methods have poor tissue penetration and tissue fluorescence, thereby making it impossible to obtain DAO spatial distributions within a region of interest *in vivo*. But, the ^{129}Xe@CB6 "OFF–ON" MRI biosensor offers an opportunity to map the DAO enzyme reaction and changes in its distribution over time *in vivo*.

To elucidate the mechanism of the enzymatic reaction between the CB6 cage and DAO, the products of this reaction were analyzed *via* mass spectrometry (MS; Fig. S2, ESI†). A peak at 70.0660 *m*/*z* corresponding to Δ1-pyrroline was found. Upon addition of DAO, ^{129}Xe Hyper-CEST NMR spectra were obtained in the same sample at different times (Fig. S4, ESI†). The intensity of the ^{129}Xe@CB6 Hyper-CEST signals at δ = 105 ppm increased gradually over time and recovered 8 days later compared with CB6 alone. The above results demonstrated that the host–guest interactions between CB6 and Put did not prevent Put from being oxidized by DAO.

Previous research has confirmed that organic ammonium could enter the cavity of CB6 and form a 1 : 1 host–guest complex.[22] Putrescine and cadaverine can inhibit the ^{129}Xe@CB6 NMR signals in solution. To confirm if the Put could take effect as expected in the biosensor, its binding affinity with CB6 was measured by ITC at the following conditions: 298 K, pH 7.2, and 20 mM NH_4OAc buffer (Fig. S3, ESI†). The result showed that the binding affinity between CB6 and Put was 2.62×10^6 ($\pm 3.66 \times 10^5$). This value is significantly greater than those reported and was a much higher value than those reported for the binding affinities between CB6 and ^{129}Xe (K^A = 500–3000 M^{-1}).[19] So, this system can be an "OFF–ON" biosensor as we expected. Moreover, Tabor's (1951) *et al.* previous research has confirmed that the aldehyde afforded as a result of the oxidation of Put undergoes subsequent condensation to form Δ1-pyrroline.[23] Δ1-pyrroline did not contain a functional group that combined with CB6. Accordingly, the ^{129}Xe@CB6 NMR signals can be lightened by DAO.

Based on the result above, the reported system was explored with HP ^{129}Xe NMR spectroscopy in buffer. First, 50 μM CB6 was dissolved in 20 mM NH_4OAc buffer (pH 7.2). Continuous wave (CW) saturation pulses were scanned over a chemical shift range of δ = 60–220 ppm in 3 ppm steps. As shown in Fig. 1(a), two saturation responses were displayed in the Hyper-CEST spectrum of CB6. One saturation response attributable to the direct saturation of free dissolved ^{129}Xe was centered at δ = 193.5 ppm, whereas the other was centered at 105 ppm, stemming from the saturation transfer of ^{129}Xe encapsulated in CB6. This result proved that the exchange kinetics of ^{129}Xe were consistent with Hyper-CEST. Upon addition of 100 μM Put to the solution and

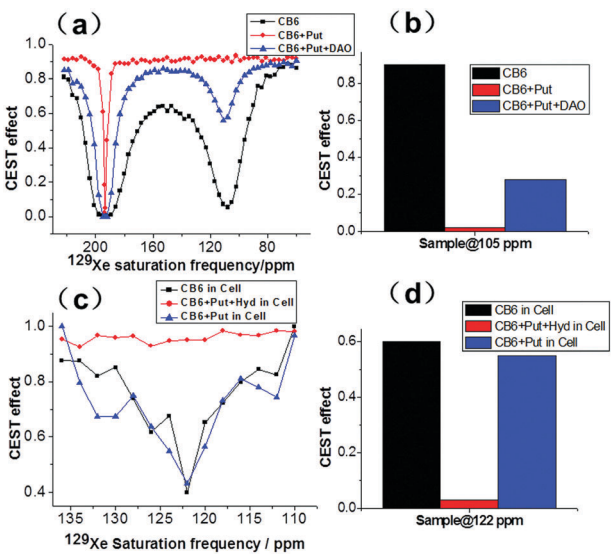

Fig. 1 Details and overview of Hyper-CEST spectra and the CEST effect in buffer and cells, with ^{129}Xe gas at δ = 0 ppm for reference. (a) Hyper-CEST spectra in buffer with only CB6, with Put, and DAO. Saturation parameters: B_1 = 6.5 μT and t_{sat} = 10 s. Conditions: 20 mM NH_4OAc, 25 °C, and pH 7.2. (b) Details of the CEST effect @105 ppm in buffer. (c) Hyper-CEST spectra in cells with only CB6 co-incubation with IVEC, with Put co-incubation with IVEC, with Put, and Hyd. Saturation parameters: B_1 = 20 μT and t_{sat} = 15 s. (d) Details of the CEST effect @122 ppm in cells.

incubation for 25 min, the ^{129}Xe@CB6 Hyper-CEST signal at δ = 105 ppm disappeared completely. Due to the strong binding of CB6@Put, the exchange was completely blocked. As shown in Fig. 1(a) and (b), when 2 mg mL^{-1} of DAO was added to the solution and co-incubated for 36 h, the ^{129}Xe@CB6 Hyper-CEST signal "turned on" because of the CB6 cavity release by the oxidization of Put. Then, CB6 was available for the interaction with ^{129}Xe. Taken together, these results indicate that DAO can have a highly sensitive and specific detection due to significant enhancement in the ^{129}Xe@CB6 Hyper-CEST signal (30% CEST effect). Moreover, the intensity of the ^{129}Xe@CB6 Hyper-CEST signal at δ = 105 ppm was found to increase gradually over time. The cavity of CB6, which was progressively released by DAO, was again occupied by ^{129}Xe (refer to Fig. S4, ESI†). Simultaneously, the signal of the dissolved ^{129}Xe Hyper-CEST at δ = 193.5 ppm widened progressively because of the off-resonance effect and release from the CB6 cavity. To reduce foam formation when bubbling ^{129}Xe in the gas mixture, 0.1% of Pluronic L-81 (by volume) was added right before the NMR and MRI measurements. To verify whether cellular DAO could be monitored using the proposed biosensor *via* ^{129}Xe NMR, the Hyper-CEST method was applied in cell studies. In the first group, CB6 (2.5 mM) was dissolved in the DMEM medium (including 10% fetal bovine serum and 1% penicillin–streptomycin), followed by incubation with the intestinal villus and epithelial cells (IVEC) in a culture flask at 37 °C. After 20 h incubation, the cells were washed and resuspended in the culture medium and the cell concentration was maintained at 3 × 10^6 cells per mL. To detect the cellular ^{129}Xe@CB6 NMR signal, a selective CW saturation pulse for 15 s with a 20 μT field was swept across the chemical shift range of 110–136 ppm in 2 ppm steps. As shown in Fig. 1(c) and (d), only one signal appeared around 122 ppm according to ^{129}Xe@CB6 in the cells. Then, 2.5 mM hydroxylamine hydrochloride (Hyd) was used to block cellular DAO in the control group to confirm whether the cellular ^{129}Xe@CB6 signal could be suppressed by Put. CB6, Put, and Hyd were incubated for 20 h in a control group. The remaining procedures were identical to those of the first group (*i.e.*, cell concentration held at 3 × 10^6 cells per mL). The cellular ^{129}Xe@CB6 Hyper-CEST signal was "turned off" which is attributed to the close combination of CB6 and Put. For comparison with the control group, CB6 (2.5 mM) and Put (5 mM) were dissolved in the DMEM medium (including 10% fetal bovine serum and 1% penicillin, streptomycin) and the remaining procedures were identical to those of the first group. Interestingly, DAO lightened the cellular ^{129}Xe@CB6 suppressed by Put, allowing for sensitive and specific detection of endogenous DAO by ^{129}Xe Hyper-CEST NMR.

In addition to the Hyper-CEST ^{129}Xe NMR analysis, the biosensor was studied by Hyper-CEST ^{129}Xe MRI. The experiments for the ^{129}Xe Hyper-CEST MRI study in 20 mM NH_4OAc buffer (pH 7.2) are shown in Fig. 2a–c, where a FLASH sequence with a 10 s, 6.5 μT CW saturation pulse was applied. The resonance frequency of the pulse was set at −83.5 ppm relative to free ^{129}Xe in the solution, and the off resonance frequency was set at 83.5 ppm. The Hyper-CEST ^{129}Xe MRI images (a) CB6, (b) CB6 + Put, and (c) CB6 + Put + DAO were obtained using a

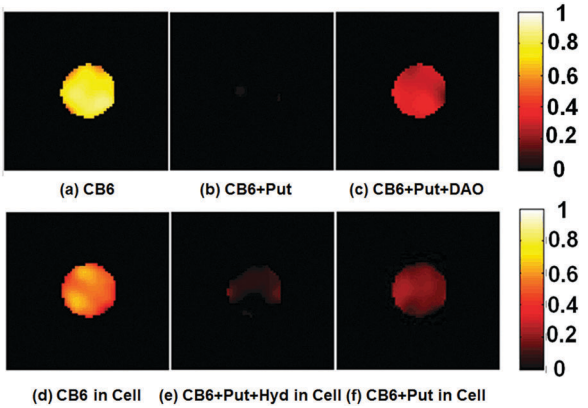

Fig. 2 Details and overview of the Hyper-CEST MRI study in buffer and cells. As shown in Hyper-CEST ^{129}Xe MRI images, (a) CB6, (b) CB6 + Put, and (c) CB6 + Put + DAO, the ^{129}Xe@CB6 Hyper-CEST signal in buffer disappeared upon the addition of 2 equivalents of Put, while the ^{129}Xe@CB6 Hyper-CEST signal appeared again upon the addition of DAO. As shown in Hyper-CEST ^{129}Xe MRI images, (d) CB6 in Cells, (e) CB6 + Put + Hyd in Cells, (f) CB6 + Put in Cells, the ^{129}Xe@CB6 Hyper-CEST signal disappeared in cells upon the addition of 2 equivalents of Put and Hyd, while the ^{129}Xe@CB6 Hyper-CEST signal in cells appeared again upon removing Hyd. Images were acquired with a matrix size of 32 × 32 point images (field of view: 2 cm × 2 cm).

FLASH sequence. The difference between images (a) and (b) in Fig. 2 shows that the ^{129}Xe@CB6 MRI signals could be completely suppressed by Put. Moreover, the difference between images (b) and (c) illustrates that DAO could be specifically detected and localized by Hyper-CEST ^{129}Xe MRI. This result demonstrated that highly sensitive and selective DAO detection could be achieved by this "OFF–ON" biosensor through a Hyper-CEST ^{129}Xe MRI method. The experiments for the ^{129}Xe Hyper-CEST MRI cell study were as follows: as shown in Fig. 2d–f, where a FLASH sequence with a 10 s, 13 μT continuous wave saturation pulse, whose resonance and off resonance frequencies were set at −71.5 and 71.5 ppm, respectively, relative to free ^{129}Xe in solution at 0 ppm, was used to obtain the ^{129}Xe Hyper-CEST MRI images of our biosensor: (d) CB6 in cells, (e) CB6 + Put + Hyd in cells, and (f) CB6 + Put in cells. Moreover, the difference between images (e) and (f) revealed that DAO in cells could be specifically detected and localized by ^{129}Xe Hyper-CEST MRI. We set 0.2× maximum value as a threshold to segment the image and interpolated it into a 64 × 64 matrix in the post processing. These results clearly demonstrate that highly sensitive and selective detection of DAO in cells can be achieved with a HP ^{129}Xe "OFF–ON" MRI biosensor. Thus, the proposed biosensor was found to extend the utility of CB6 for an ultrasensitive ^{129}Xe NMR biosensor.

The Hyper-CEST response of CB6 was better compared to that of Cry-A.[24] This response rendered CB6 more attractive and important for a variety of applications, including MRI and NMR detection. The results represented here prove that the ^{129}Xe@CB6 NMR signals can be entirely inhibited by a substrate until a specific enzymatic reaction occurs. These signals appear again when the CB6 cavity is emptied. The proposed biosensor can be used to identify endogenous biomarkers in

IVEC, enabling its easy handling in laboratories and circumventing tedious synthetic procedures. Consequently, this project represents prospects for CB6 that are to be increasingly applied in ^{129}Xe NMR detection, together with multi-modality imaging, drug delivery, and ratiometric probes. Our future research will be focused on the search for other CB6 guests that could be used with our model for its application in the detection of a wide range of diseases and *in vivo* detection.

This work was financially supported by the National Natural Science Foundation of China (81227902, 81625011), National Key R&D Program of China (2016 YFC 1304704) and the Key Research Program of Frontier Sciences, CAS (QYZDY-SSW-SLH018); X. Zhou thanks the National Program for Special Support of Eminent Professionals (National Program for Support of Top-notch Young Professionals).

Conflicts of interest

There are no conflicts to declare.

Notes and references

1 (*a*) Y. Gandon, D. Olivie, D. Guyader, C. Aube, F. Oberti and V. Sebille, *Lancet*, 2004, **363**, 357; (*b*) C. A. Nienaber, Y. Kodolitsch, V. Nicolas, V. Siglow, A. Piepho, C. Brockhoff, D. H. Koschyk and R. P. Spielmann, *N. Engl. J. Med.*, 1993, **328**, 1; (*c*) P. A. Bottomley, *Science*, 1985, **229**, 769; (*d*) B. Leo, Y. Liu, C. Dong, X. Chen, X. Zhang, X. Diao, G. Yang, J. Liu, S. Yao, H. Li, J. Yuan, S. Li, X. Le, Y. Lin and W. Zeng, *Neurocomputing*, 2017, **253**, 169.

2 J. A. Finbloom, C. C. Slack, C. J. Bruns, K. Jeong, D. E. Wemmer, A. Pines and M. B. Francis, *Chem. Commun.*, 2016, **52**, 3119.

3 (*a*) E. L. Que, E. J. New and C. J. Chang, *Chem. Sci.*, 2012, **3**, 1829; (*b*) G. Liu, Y. Li and M. D. Pagel, *Magn. Reson. Med.*, 2007, **58**, 1249; (*c*) J. Alvarez-Pérez, P. Ballesteros and S. Cerdán, *Magn. Reson. Mater. Phys., Biol. Med.*, 2005, **18**, 293; (*d*) M. G. Shapiro, T. Atanasijevic, H. Faas, G. G. Westmeyer and A. Jasanoff, *Magn. Reson. Imaging*, 2006, **24**, 449.

4 M. Muñoz Úbeda, F. Carniato, V. Catanzaro, S. Padovan, C. Grange, S. Porta, C. Carrera, L. Tei and G. Digilio, *Chem. – Eur. J.*, 2016, **22**, 7716.

5 (*a*) E. Terreno, C. Boffa, V. Menchise, F. Fedeli, C. Carrera, D. Castelli, G. Digilio and S. Aime, *Chem. Commun.*, 2011, **47**, 4667; (*b*) K. Matsuo, R. Kamada, K. Mizusawa, H. Imai, Y. Takayama, M. Narazaki, T. Matsuda, Y. Takaoka and I. Hamachi, *Chem. – Eur. J.*, 2013, **19**, 12875.

6 (*a*) T. Chauvin, P. Durand, M. Bernier, H. Meudal, B. T. Doan, F. Noury, B. Badet, J. C. Beloeil and É. Tóth, *Angew. Chem., Int. Ed.*, 2008, **47**, 4370; (*b*) J. Zhou, J. F. Payen, D. A. Wilson and R. J. Traystman, *Nat. Med.*, 2003, **9**, 1085; (*c*) K. Ward and R. Balaban, *Magn. Reson. Med.*, 2000, **44**, 799.

7 (*a*) N. J. Goffeney, W. Bulte, J. Duyn and L. H. Bryant, *J. Am. Chem. Soc.*, 2001, **123**, 8628; (*b*) Y. Wang and I. J. Dmochowski, *Acc. Chem. Res.*, 2016, **49**, 2179; (*c*) P. Berthault, A. Bogaert-Buchmann, H. Desvaux, G. Huber and Y. Boulard, *J. Am. Chem. Soc.*, 2008, **130**, 16456.

8 (*a*) P. Nikolaou, A. M. Coffey, L. L. Walkup, B. M. Gust, N. Whiting, H. Newton, S. Barcus, I. Muradyan, M. Dabaghyan and G. D. Moroz, *Proc. Natl. Acad. Sci. U. S. A.*, 2013, **110**, 14150; (*b*) N. Kotera, N. Tassali, E. Léonce, C. Boutin, P. Berthault, T. Brotin, J. P. Dutasta, L. Delacour, T. Traoré and D. A. Buisson, *Angew. Chem., Int. Ed.*, 2012, **51**, 4100; (*c*) T. Meldrum, K. L. Seim, V. S. Bajaj, K. K. Palaniappan, W. Wu, M. B. Francis, D. E. Wemmer and A. Pines, *J. Am. Chem. Soc.*, 2010, **132**, 5936.

9 (*a*) G. K. Seward, Y. Bai, N. S. Khan and I. J. Dmochowski, *Chem. Sci.*, 2011, **2**, 1103; (*b*) Y. Bai, P. A. Hill and I. J. Dmochowski, *Anal. Chem.*, 2012, **84**, 9935; (*c*) I. Ruset, S. Ketel and F. Hersman, *Phys. Rev. Lett.*, 2006, **96**, 053002.

10 (*a*) R. Jiménez-Martínez, D. J. Kennedy, M. Rosenbluh, E. A. Donley, S. Knappe, S. J. Seltzer, H. L. Ring, V. S. Bajaj and J. Kitching, *Nat. Commun.*, 2014, **5**, 3908; (*b*) S. Patz, F. W. Hersman, I. Muradian, S. Ketel, F. Jacobson, G. P. Topulos, H. Hatabu and J. P. Butler, *Eur. J. Radiol.*, 2007, **64**, 335.

11 (*a*) M. Springuel-Huet, J. Bonardet, A. Gédéon and J. Fraissard, *Langmuir*, 1997, **13**, 1229; (*b*) W. Zhang, C. I. Ratcliffe, I. L. Moudrakovski and C. Y. Mou, *Anal. Chem.*, 2005, **77**, 3379.

12 (*a*) Q. Guo, Q. Zeng, W. Jiang, X. Zhang, Q. Luo, X. Zhang, L. S. Bouchard, M. Liu and X. Zhou, *Chem. – Eur. J.*, 2016, **22**, 3967; (*b*) P. Tallavaara, V. V. Telkki and J. Jokisaari, *J. Phys. Chem. B*, 2006, **110**, 21603; (*c*) H. Long, M. Luzar, H. Gaede, R. Larsen, J. Kritzenberger, A. Pines and G. Crawford, *J. Phys. Chem.*, 1995, **99**, 11989.

13 (*a*) B. Jagadeesh, A. Prabhakar, M. R. Rao, C. Murty, V. Pisipati, A. Kunwar and C. Bowers, *J. Phys. Chem. B*, 2004, **108**, 11272; (*b*) B. A. Riggle, Y. Wang and I. J. Dmochowski, *J. Am. Chem. Soc.*, 2015, **137**, 5542; (*c*) P. Berthault, H. Desvaux, H. Wendlinger, M. Gyejacquot, A. Stopin, T. Brotin, J. P. Dutasta and Y. Boulard, *Chem. – Eur. J.*, 2010, **16**, 12941.

14 (*a*) L. Schröder, T. Meldrum, M. Smith, T. J. Lowery, D. E. Wemmer and A. Pines, *Phys. Rev. Lett.*, 2008, **100**, 257603; (*b*) D. N. Sears and C. J. Jameson, *J. Chem. Phys.*, 2003, **119**, 12231; (*c*) C. Witte, V. Martos, H. M. Rose, S. Reinke, S. Klippel, L. Schröder and C. P. Hackenberger, *Angew. Chem., Int. Ed.*, 2015, **54**, 2806.

15 (*a*) J. Döpfert, C. Witte, M. Kunth and L. Schröder, *Contrast Media Mol. Imaging*, 2014, **9**, 100; (*b*) C. Witte, M. Kunth, F. Rossella and L. Schröder, *J. Chem. Phys.*, 2014, **140**, 084203; (*c*) L. Schröder, T. J. Lowery, C. Hilty, D. E. Wemmer and A. Pines, *Science*, 2006, **314**, 446.

16 (*a*) L. Schröder, L. Chavez, T. Meldrum, M. Smith, T. J. Lowery, D. E. Wemmer and A. Pines, *Angew. Chem., Int. Ed.*, 2008, **47**, 4316; (*b*) M. Schnurr, C. Witte and L. Schröder, *Phys. Chem. Chem. Phys.*, 2013, **15**, 14178; (*c*) O. Taratula and I. J. Dmochowski, *Curr. Opin. Chem. Biol.*, 2010, **14**, 97; (*d*) R. M. Fairchild, A. I. Joseph, K. T. Holman, H. A. Fogarty, T. Brotin, J. P. Dutasta, C. L. Boutin, G. Huber and P. Berthault, *J. Am. Chem. Soc.*, 2010, **132**, 15505.

17 (*a*) T. K. Stevens, K. K. Palaniappan, R. M. Ramirez, M. B. Francis, D. E. Wemmer and A. Pines, *Magn. Reson. Med.*, 2013, **691**, 1245; (*b*) T. Brotin and J. P. Dutasta, *Chem. Rev.*, 2008, **109**, 88; (*c*) M. Luhmer, B. M. Goodson, Y. Q. Song, D. D. Laws, L. Cyrier, M. C. Kaiser and A. Pines, *J. Am. Chem. Soc.*, 1999, **121**, 3502.

18 (*a*) C. Marquez and W. M. Nau, *Angew. Chem., Int. Ed.*, 2001, **40**, 3155; (*b*) R. N. Dsouza, U. Pischel and W. M. Nau, *Chem. Rev.*, 2011, **111**, 7941; (*c*) J. Mohanty, A. Bhasikuttan, W. Nau and H. Pal, *J. Phys. Chem. B*, 2006, **110**, 5132; (*d*) M. Floreaa and W. M. Nau, *Angew. Chem., Int. Ed.*, 2011, **50**, 9338.

19 (*a*) Y. Wang, B. W. Roose, J. P. Philbin, J. L. Doman and I. J. Dmochowski, *Angew. Chem., Int. Ed.*, 2016, **55**, 1733; (*b*) M. Schnurr, J. Döpfert, L. Schröder and A. Hennig, *Angew. Chem., Int. Ed.*, 2015, **54**, 13444; (*c*) C. C. Slack, J. A. Finbloom, K. Jeong, C. J. Bruns, D. E. Wemmer, A. Pines and M. B. Francis, *Chem. Commun.*, 2017, **53**, 1076; (*d*) J. Döpfert, M. Schnurr, M. Kunth, H. M. Rose, A. Hennig and L. Schröder, *Magn. Reson. Chem.*, 2018, **56**, 679.

20 (*a*) E. Music, M. Silar, P. Korosec, M. Kosnik and M. Rijavec, *Wien. Klin. Wochenschr.*, 2013, **125**, 239; (*b*) C. H. Jin, C. S. Ick, K. H. One, P. C. Wook and L. C. Heon, *Ann. Dermatol.*, 2013, **25**, 189; (*c*) W. U. Schmidt, J. Sattler, R. Hesterberg, T. Zoedler, H. Sitter and W. Lorenz, *Agents Actions*, 1990, **30**, 267; (*d*) B. Elmfors, N. Tryding and G. Tufvesson, *BJOG*, 1974, **81**, 361.

21 W. M. Nau, G. Ghale, A. Hennig, H. Bakirci and D. M. Bailey, *J. Am. Chem. Soc.*, 2009, **131**, 11558.

22 (*a*) H. Zhang, T. A. Ferrell, M. C. Asplund and D. V. Dearden, *Int. J. Mass Spectrom.*, 2007, **265**, 187; (*b*) S. J. Barrow, S. Kasera, M. J. Rowland, J. del Barrio and O. A. Scherman, *Chem. Rev.*, 2015, **115**, 12320.

23 (*a*) J. E. Amoore, L. J. Forrester and R. G. Buttery, *J. Chem. Ecol.*, 1975, **1**, 299; (*b*) B. Bolmstedt and R. Tham, *Acta Physiol. Scand.*, 1959, **45**, 152; (*c*) H. Tabor, *J. Biol. Chem.*, 1951, **188**, 125.

24 M. Kunth, C. Witte, A. Hennig and L. Schröder, *Chem. Sci.*, 2015, **6**, 6069.